Synchrotron radiation micro-computed tomography for the investigation of finishing treatments in historical bowed string instruments: Issues and perspectives

Synchrotron radiation micro-computed tomography for the investigation of finishing treatments in historical bowed string instruments: issues and perspectives

Giacomo Fiocco[(a,b)], Tommaso Rovetta[(a,c)], Marco Malagodi[(a,d)], Maurizio Licchelli[(a)], Monica Gulmini[(b)]*, Gabriele Lanzafame[(e)], Franco Zanini[(e)], Alessandro Lo Giudice[(f)], Alessandro Re[(f)]

[(a)] *Laboratorio Arvedi di Diagnostica Non Invasiva, CISRiC, Università degli Studi di Pavia, Via Bell'Aspa 3, 26100 Cremona, Italy*
[(b)] *Dipartimento di Chimica, Università di Torino, Via Pietro Giuria 5, 10125, Torino, Italy*
[(c)] *Dipartimento di Fisica, Università degli Studi di Pavia, Via Bassi 6, 27100 Pavia, Italy*
[(d)] *Dipartimento di Musicologia e Beni Culturali, Corso Garibaldi 178, 26100 Cremona, Italy*
[(e)] *Elettra-Sincrotrone Trieste S.C.p.A., S.S. 14 km 163.5, 34194 Basovizza, Trieste, Italy*
[(f)] *Dipartimento di Fisica, Università di Torino and INFN, Sezione di Torino, Via Pietro Giuria 1, 10125 Torino, Italy*

* corresponding author: monica.gulmini@unito.it

Short title: SR-micro-CT to investigate finishing treatments in bowed string instruments

Abstract
Coating systems in historical bowed string instruments are often multi-layered structures, where several inorganic and organic materials are variously combined. The methods to characterise such complex systems normally require samples to be detached from the artwork, whereas Synchrotron Radiation micro-Computed Tomography (SR-micro-CT) may reveal - through a non-invasive approach - procedures and materials employed by the ancient violin makers. Since the application of SR-micro-CT for the investigation of the finishing layers in historical bowed string instruments is still unexplored, the experimental settings were optimized for the detection of the main features expected in the finishing layers of an historical instrument. In this work, two sets of mock-ups mimicking the finishing layers of historical instruments and a large fragment removed from a damaged cello by Andrea Guarneri were scanned. By considering the SR-micro-CT data, and data obtained by previous micro-invasive analyses, the merits of reconstructed volumes and virtual slicing in investigating the layered structures have been highlighted and discussed. The developed procedures enabled the detection of the main morphological features of the overlapping layers, producing a valuable, non-invasive insight into the structure of the coating systems.

1. Introduction

The smooth and shiny varnish of an historical violin is the most perceivable portion of a complex multi-layered coating system, which may contain a variety of inorganic and organic materials [1]. All these materials are involved in the finishing treatments of the musical instrument, enhancing the aesthetic features of the wood, protecting the object from wear and influencing the tonal features of the sound [2].
Nowadays, scientific investigation represents a powerful tool to rediscover the lost materials and methods adopted in the finishing treatments employed by early Masters of violin making, which were traditionally passed down orally to apprentices, and forgotten when the workshop's activity ceased. Scientists have invested effort in setting up new analytical schemes and innovative techniques and procedures for probing the instruments, in order to obtain relevant information for properly identifying the context of production [3-5]. The main focus has been the characterization of the Cremonese varnish and of the other materials involved in the finishing treatments [6]. However, the in-depth coating system characterisation in bowed string instruments is - in most cases - rather challenging. In fact, the identification of the variety of substances that may be present - normally distributed over large concentration intervals - needs the recovering of spatially resolved information and the chemical characterisation of the constituents of each layer. This task can be tackled by combining the results obtained from a set of approaches based on various instrumental techniques.
Recently, a few research teams have considered the development of systematic protocols for the scientific investigation of bowed string instruments. The characterization of these materials is generally carried out by non-invasive spectroscopic analyses - such as X-Ray Fluorescence (XRF), Fourier Transform Infrared spectroscopy (FTIR) in reflection modality, Raman spectroscopy - or by micro-analytical techniques - such as micro-FTIR or Scanning Electron Microscopy coupled with Energy Dispersive X-ray analysis (SEM-EDX) - performed on single grains dispersed in the finishing layers [7-11].

Thanks to the most recent results concerning historical musical instruments, it is presently well known that different mineral grounds - such as calcium sulphates, calcium carbonates and silicates [3,5] - dispersed in a proteinaceous binder - such as casein or animal glues - were widely used to fill up the wood pores before the varnish application. These materials were probably applied in many superimposed coats giving a ground layer that produced smoothed and sealed surfaces. Over the ground layer, one or more varnish layers were then applied [12]. Basically, violin varnishes are obtained through natural organic film-making materials such as di- or tri-terpenic natural resins dissolved in alcohol, volatile oils or siccative oils. The colour of the varnish – which may cover or enhance the original colour of the wood – derives from natural dyes or from organic and inorganic pigments intentionally added to the mixture in order to bring out a specific hue [3,10,13,14].
Samples from intact instruments are normally not available for the scientific investigation, therefore the research is presently focused on testing new strategies aimed at enlarging the information that can be obtained through non-invasive instrumental approaches.
Under this scenario, synchrotron-based methods are among the most promising candidates to catch a non-invasive insight into the secrets of early violin makers, as they enable spatially resolved micro-analyses for detecting organic and inorganic components directly on the artwork [15]. The broad energy spectrum of the high-flux and high-brilliance radiation produced by a synchrotron is in fact perfectly exploitable in a wide set of spectroscopic techniques, provided that the artwork can be properly arranged to detect the analytical signals. Moreover, X-rays can be exploited for computed tomography (CT) application to obtain high-resolution 3D reconstructions of the morphological structure of the instrument.
CT is a well-established technique for the morphological characterization of bowed string instruments, and it has been extensively used by modern violin-makers and acoustic scientists in the last decade. Since the first feasibility studies by Sirr and Waddle in 1997 [16] performed by a clinical CT system (i.e. the computed tomographic system currently used in hospitals), some authors described the application of the CT-scan for a non-invasive observation of the entire bowed string instrument. CT-scans have allowed to detect damages and restorations occurred over time [17]. The new possibilities offered by the last generation synchrotron sources, together with the development of novel X-ray detectors and faster computers, have significantly increased the application of X-ray microtomography in the tangible cultural heritage domain [18]. The interesting characteristics of synchrotron radiation (SR) are the continuous spectrum, extending from infrared to hard X-rays, the high intensity, and the high spatial coherence of the X-ray beam. These features allow fast exposure times, tuning photon energy as a function of sample characteristics and using digital subtraction techniques [19]. In addition, monochromaticity and high collimation of the beam reduce artefacts and increase quality of data analysis. Furthermore, phase-sensitive imaging techniques using highly coherent, hard X-rays from third-generation synchrotron sources have the additional advantage of enabling samples imaging even if very low absorption contrast is expected, such as for light-element adhesives and consolidants [20]. SR-micro-CT has been extensively applied to bowed stringed instruments since 2010 at Elettra synchrotron laboratory (Trieste, Italy) [21-23], in order to extract morphological information about the structure of historical violins with spatial resolutions between 9 and 50 μm. The geometry of the experimental hutch allows to perform the experiments on the entire instrument in a controlled environment (RH 53% ± RH 2% and 26°C). The information that can be extracted ranges from the presence of damages (usually concealed with glue, filler materials, retouches or varnish) to the woodworms infestation, from the manufacturing details to 3D data for dendrochronology.
In this work, the attention has been focused on the coating system and a SR-micro-CT procedure has been developed in order to obtain 3D volumes and 2D slices of micrometric layered systems such those encountered in historical bowed string instruments. Despite the previous papers have already suggested that SR-micro-CT could be possibly employed successfully for this aim [17], the topic has not been considered carefully yet. Therefore, mock-ups mimicking the coating systems of historical instruments have been considered here in the first step of our research, in order to optimise the instrumental settings, boost the spatial resolution and define reconstruction parameters.
The merits of the images obtained on the mock-ups for the investigation of the layers sequence and of the morphology of the dispersed particles have been evaluated. Moreover, the sensitivity of the CT-scan has been tested to assess the possibility to distinguish different organic layers.
The procedure developed on mock-ups has been then tested on a large fragment detached from a cello produced in the 17th century by the Italian master Andrea Guarneri.
In order to outline a robust interpretation frame for the non-invasive SR-micro-CT approach, information obtained by micro-invasive analyses have been also considered here for evaluating the merits of the reconstructed volumes and virtual slicing in investigating layered complex structures.

The work is part of a wider project devoted to develop scientific non-invasive procedures to investigate the finishing treatments on historical instruments and to enlarge the knowledge about the production methods adopted by the ancient violin makers through the study of their still-surviving instruments.

2. Materials and methods

2.1 Mock-ups preparation

Two sets of mock-ups (5 cm x 1,7 cm x 1 cm) were prepared, in order to simulate the main typologies of coating systems that can be encountered in historical instruments [24]. Commercially available organic and inorganic materials were selected according to their use in the finishing processes of historical musical instruments.

The first set encompasses three mock-ups (Ground1-3) and has been prepared in order to evaluate whether CT analysis would allow the identification of different mineral grounds through the visualization of dimensions and morphologies of the embedded inorganic particles. Three different inorganic powders were considered. Maple wood slabs were ground coated employing dispersions of calcium sulfate $CaSO_4 \cdot 2H_2O$ (Ground1), calcium carbonate $CaCO_3$ (Ground2) and kaolinite $Al_2Si_2O_5(OH)_4$ (Ground3) in a solution of ammonium caseinate spread by brush. Then, a layer of a linseed oil-colophony varnish (OCV) was applied in two coats upon each ground layer, using a bar film applicator.

The second set (Madder1,2) was instead used to highlight lightweight colourant particles - such as alum-based madder lake - dispersed in different binders. “Lake” refers to pigments made by an organic dye supported on an inorganic substrate. According to traditional recipes [25], the substrate is normally hydrated aluminum oxide formed by addition of a basic reagent to a solution of aluminum potassium sulfate dodecahydrate (potash alum). Due to a number of issues [14] lakes are normally difficult to be detected in complex coating systems such as those of bowed string instruments. The sensitivity of SR-micro-CT scan was thus tested for the detection of lakes. For this experiment, maple wood slabs were ground coated with ammonium caseinate and then covered by a layer of OCV. The pigment was dispersed in the ground layer of the first mock-up (Madder1), while it was spread in the varnish of the second one (Madder2).

Material suppliers and procedures for the preparation of the first and the second set are respectively reported in [6] and [14]. The sequences of the layers in the mock-ups are summarized in Table 1.

Table 1. Layer sequences for the selected coating systems. AC = ammonium caseinate; OCV = linseed oil-colophony varnish (two coats). The ground layer was obtained by spreading one coat of the AC primer (without the dispersed inorganic powder) and a second coat of the primer with the dispersed particles. Only in Madder2 the ground layer was prepared with one coat without particles and two further coats with the dispersed madder lake.

	Mock-ups				
	Ground1	**Ground2**	**Ground3**	**Madder1**	**Madder2**
Varnish layer	OCV	OCV	OCV	OCV	OCV + Madder lake
Ground layer	AC + calcium sulfate	AC + calcium carbonate	AC + kaolinite	AC + Madder lake	AC
Support material	Maple wood	Maple wood	Maple wood	Maple wood	Maple wood

2.2 The case study: a fragment from a cello by Andrea Guarneri

In addition to the mock-up sets, a large fragment (20,1 cm x 3,8 cm x 0,38 cm) removed from a damaged cello was subjected to the SR-micro-CT scan. The fragment was selected from the Sgarabotto’s collection, which is made up by many parts of bowed string instruments restored during the 20th century by Gaetano and Pietro Sgarabotto [5,11]. The collection includes fragments from some instruments attributed to the most representative Italian violin-makers active between the 17th and the 19th century (i.e. Gasparo da Salò, Nicola Amati, Andrea Guarneri, Lorenzo Guadagnini, Luigi Baioni).

The here-selected fragment was obtained from the top plate of a cello made by Andrea Guarneri (1626-1698) during the second half of the 17th century. The coating system on the fragment was previously characterized by a multi-analytical approach as reported in Fiocco et al. [5]. In that work, non-invasive and micro-invasive techniques (XRF, micro-FTIR and SEM-EDX), preceded by a preliminary observation by Optical Microscopy (OM) in visible and UV light, revealed a complex stratigraphy with three subsequent layers. White particles - identified as gypsum - were dispersed in a 15 µm thick proteinaceous binder spread directly on the wood substrate. The UV-light revealed the dark red-violet fluorescence of a further layer (about 10 µm thick) applied over the ground layer, possibly embedding silicates, feldspars, and ochres. The upper varnish was prepared

with a natural resin spread in a 20 μm thick layer. A dispersion of micrometric red particles, probably related to the intentional use of red ochres, was detected within the varnish layer.

2.3 Optical, Electron and Stereo Microscopy

In order to obtain information that will guide the interpretation of the SR-micro-CT images, the main features of the mock-ups involved in this work were investigated by OM and SEM on small samples detached from them. The collected samples were embedded in epoxy resin (Epofix Struers and Epofix Hardener with ratio 15:2), cut as cross sections using a diamond blade and than polished with silicon carbide fine sandpapers (800–4000 mesh). Both the mock-ups and the polished cross-sections were observed through an Olympus BX51TF polarized light optical microscope equipped with Olympus TH4-200 (visible light) and Olympus U-RFL-T (UV radiation) lamps. Imaging at higher magnifications was performed by a FE-SEM Tescan Mira 3XMU-series SEM-EDX (Brno, Czech Republic), set with an accelerating voltage of 20 kV in high vacuum and equipped with a Bruker Quantax 200 Energy-Dispersive X-ray spectrometer (Billerica, MA, USA). Surface details were observed by an Olympus SZX10 stereomicroscope (Tokyo, Japan) equipped with an Olympus DP73 camera and a Schott KL1500 illuminator.

2.4 Synchrotron X-ray microtomography setup and 3D reconstruction

The three-dimensional study of the mock-ups and of the micromorphology of the fragment were performed by high-resolution SR-micro-CT in phase-contrast mode [26] at the SYRMEP beamline of the Elettra synchrotron laboratory (Trieste, Italy). A polychromatic X-ray beam delivered by a bending magnet source illuminated the sample in transmission geometry. Regarding the white beam, filters (1.5 mm Si + 1 mm Al) were used to suppress the contribution of low energies in the beam spectrum. With this configuration the average beam energy resulted to be about 28 keV. The sample-to-detector distance was set at 150 mm. For each experiment, 1800 projections were recorded rotating the sample continuously over an angle of rotation of 180 degrees, with an exposure time/projection of 0.25 s. The detector used was an air-cooled, 16 bit, sCMOS camera (Hamamatsu C11440-22C) with a 2048 × 2048 pixels chip. Measurements were carried out with an effective pixel size of the detector set at 1 × 1 μm^2 yielding a maximum field of view of about 2.4 × 2.4 mm^2.

The reconstruction of the 2D tomographic slices was done with the Syrmep Tomo Project (STP) house software suite [27]. Different combinations of the filters available in the STP software were applied to the datasets, in order to reduce ring artefacts caused by detector inhomogeneity [28]. The consistency of the morphological analysis was improved applying a single-distance phase-retrieval algorithm [29] based on the Transport of Intensity Equation (TIE) to the sample projections. This can be done by computing the complex refractive index of the samples $n = 1 - \delta + i\beta$, (where δ is the real and β the imaginary part, related to phase and absorption distribution of the sample, respectively). A constant ratio $\gamma = \delta / \beta = 151$ was determined to be the best suitable for the investigated samples. Phase-retrieval, in combination with the Filtered Back-Projection algorithm [30], allowed to obtain the 3D distribution of the complex refraction index of the imaged samples in order to reduce edge-enhancement effect at sample borders, preserving the morphology of the smallest features.

The stack of slices was imported in VGStudio Max 2.2 from Volume Graphics: it was then used both for the 3D rendering and segmentation (manual thresholding) of the volumes.

3. Results and discussion

3.1 Mock-ups

After the reconstruction of the mock-up volumes (Fig. 1a), the merits of the technique have been explored by evaluating which features of the complex coating system can be recovered by the SR-micro-CT approach.

The wood represents the largest part of the scanned volume, and longitudinal tracheids and rays are evident in the reconstructed volumes. Nevertheless, the arrangement of cells in the tissue of the wood is not considered here, as the research focuses on the finishing layers upon it.

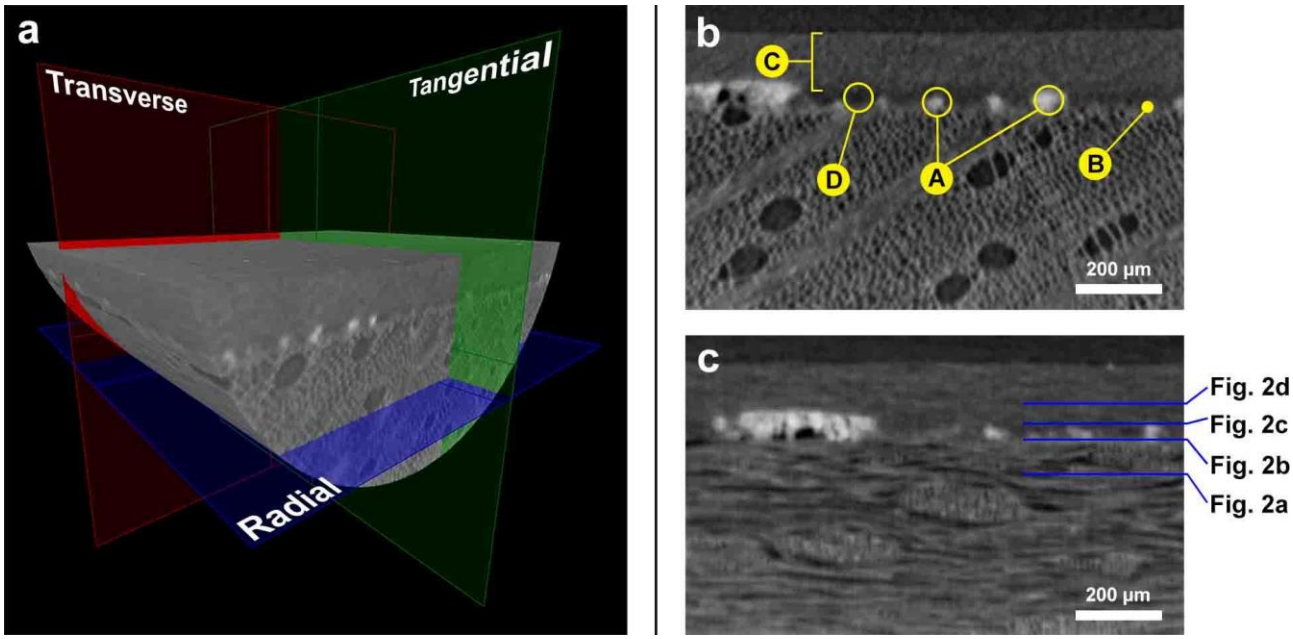

Figure 1. a) Volume rendering for Ground 1 mock-up, with planes for the virtual slicing. These planes have been selected in order to produce images of radial, tangential and transverse sections of the wood; b) transverse slice from Ground1. Particles of calcium sulphate (A), the proteinaceous ground layer (B) and the OCV layer (C) are indicated. The thin dark layer discussed in the text is also highlighted (D); c) tangential slice from Ground1. Planes for radial slices shown in Fig. 2 are reported.

Transverse and tangential views (Fig. 1b,c) have been considered as a starting point, as they can be compared with images obtained when cross sections are physically prepared. It is evident that an added value of the SR-micro-CT is represented by the non-invasive virtual slicing of the scanned volume, which offers a more representative picture of the samples.

The presence of dispersed particles embedded in the organic binder of the ground layer is evident, as they appear much brighter in greyscale images. Besides the evidence of the particles just above the wood surface, the presence of two layers of slightly different materials, such as the proteinaceous binder of the ground layer and the OCV, is barely noticeable in the slices. The ground layer appears very thin and slightly brighter than the wood, and lays directly on it (Fig 1b,c). In some of the CT-slices (Fig. 1b) it is evident instead a dark layer at the ground-to-varnish interface. This apparent layer is discussed below by comparing the image of a virtual slice with the one obtained under the optical microscope for an embedded cross-section. CT-slices allow us to measure the thickness of the ground layer (some 20 µm) and of the OCV (about 150 µm).

More information derives from radial slices (Fig. 2a-d), which are normally not obtained as physical sections to be observed under a microscope.

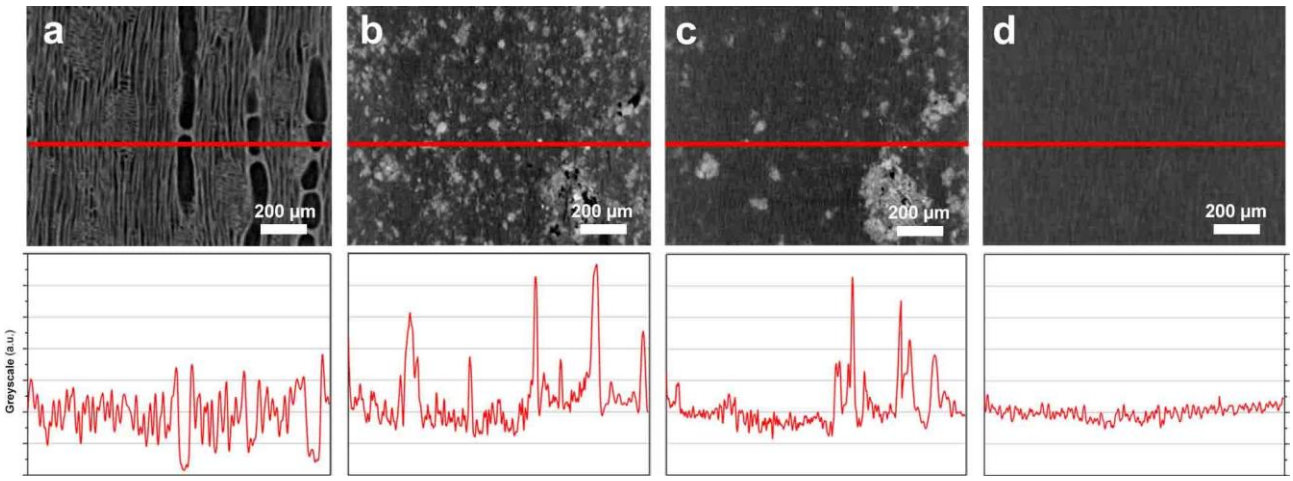

Figure 2. Radial slices from Ground1 (slice planes are reported in Fig. 1c) and greyscale profiles for the reported red lines; a) porous wood under the coating system; b) ground layer embedding the calcium sulphate particles. The presence of binders with different radiopacity is highlighted in the greyscale profile; c) aggregates of calcium sulphate sticking out of the ground layer into the varnish; d) transparent varnish layer.

Radial slices show the wood substrate (Fig. 2a), the ground layer embedding the inorganic particles and clogging up the wood pores (Fig. 2b), the dispersion of the inorganic particles with larger aggregates that extend into the varnish layer (Fig. 2c) and the transparent OCV topping the system (Fig. 2d). The sequence of the radial slices gives an excellent view of the distribution of the particles on the surface, highlighting their mean concentration, their size, and their tendency to be present in aggregates. It is evident that thinner particles are present in the ground layer (Fig. 2b), while larger aggregates tend to remain on the top of the proteinaceous layer and to be partially embedded in the varnish layer (Fig. 2c). In this sequence, the greyscale profile also allow us to highlight the presence of a further material - other than the varnish - embedding the particles at the wood-coating interface; the ground layer and the varnish layer show in fact two different levels of brightness. Although barely perceivable in the image, the difference is highlighted by the greyscale profile of Fig. 2b. In order to offer a quantitative picture of the situation, greyscale levels for $19.2 \cdot 10^3$ pixels in the brighter area (mean value=67.5, st. deviation=6.3) and for $19.2 \cdot 10^3$ pixels in the darker area (mean value=45.5, st. deviation=5.7) were selected, focussing on spots with no visible inclusion. XLSTAT software was then employed to evaluate the significance of the difference of brightness observed in Fig. 2b. Each set was subjected to Shapiro-Wilk normality test, which rejected the null hypothesis H0 (the variable from which the set of data was extracted follows a Normal distribution) for a significance level of 0.05. As a consequence, a non-parametric test (Mann-Withey's U test) was selected for comparing the two sets of data. The test lead us to rejected the null hypothesis H0 (the data have been extracted from a same population) for a significance level of 0.05 and to statistically validate the statement that the brightness of the binder is higher in the right part of the profile in Fig 2b and lower in the left part. The whole sequence suggests that the material appearing brighter is related to the proteinaceous ground layer, whereas the OCV appears darker, thus confirming the picture already emerged, although less evident, from transverse and tangential virtual slices.

The volume renderings obtained from all the Ground1-3 mock-ups (reported as supplementary information, Fig. S1) indicate that no information can be actually obtained on the nature of the embedded particles, as both morphology and differences in the greyscale level among the three inorganic powders (i.e. calcium sulphate, calcium carbonate, and kaolinite) are too poorly resolved to be conclusive.
A different situation refers to the second set of mock-ups, where a madder lake is present in the ground layer (Madder1) or in the varnish layer (Madder2). The image of the cross section of an embedded sample from Madder1 observed through the OM under UV illumination (Fig. 3a) is compared with tangential and transversal virtual slices (Fig. 3b,c). Layers A and B (Fig. 3a,b) are thinner in these mock-ups (less than 10 µm for the ground layer and about 40 µm for the OCV) and it is barely possible to recognize the presence of the proteinaceous ground layer sealing the wood porosity. The presence of particles of significantly higher brightness (Fig. 3b, particles C) is evident by considering the whole set of the tangential and transverse virtual slices.
The detection of the dispersed lake particles is instead difficult in transverse slices, as their brightness is not substantially different from the one of the dispersing agent (Fig. 3b, particles D); nevertheless, they are visible in the images obtained for both Madder1 and Madder2. Actually, the distribution of the madder particles is not limited to the thin ground layer in Madder1, and in both of them the pigment is dispersed within the entire coating system.
Moreover, Fig. 3a shows the varnish layer splitted into two parts, and only the upper one yield a yellowish fluorescence characteristic of the dry linseed oil. It is reasonable to assume that these two parts shall be related to the two varnish coats that have been employed to obtain the whole varnish layer. The same information derives from transverse and tangential virtual slices (Fig. 1 and Fig. 3), where the layer above the proteinaceous binder appears darker than the outer part of the varnish, with different thickness observed in OM and SR-micro-CT virtual slices, that could be related to the ongoing polimerization process.

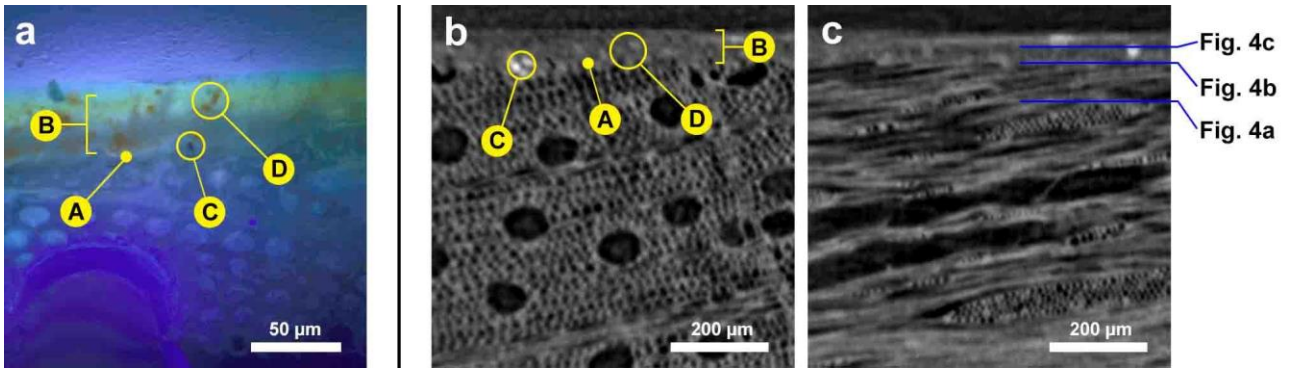

Figure 3. a) Polished cross section of a sample detached from Madder1 observed through the OM under UV light. The ground (A) and varnish (B) layers are indicated. The varnish is splitted into an upper part showing a yellowish fluorescence and a lower, less fluorescent one. Black (C) particles and evident red particle of lake (D) are also visible; b) transverse virtual slice from Madder1. The ground (A) and OCV (B) layers are indicated, and brighter particles (C) are also visible. D indicates the madder lake particles, which are barely distinguished from the embedding agent; c) tangential slide from Madder1. Planes for radial slices shown in Fig. 4 are reported.

In fact, the possibility of detecting subsequent coats within the varnish is lost for ancient varnishes, as differences has not been detected under the OM neither in artificially aged mock ups [14] nor in the varnish of historical bowed string instruments [5].
The inspection of radial slices (Fig. 4a-c) is illuminating for getting a realistic picture of the distribution of the particles within the different layers of the coating system. By following the morphology of the finishing layers from the wood to the varnish surface it is possible to disclose that the brighter particles are most probably related to the wood pre-treatment performed with sandpapers before spreading the ground layer, as some of them are inserted in the superficial porosity of the wood or in the first part of the ground layer (Figure 4b). A large number of light-grey particles are instead dispersed in the coating system and they are therefore recognized as the lake particles (Figure 4c). The presence of different particles (red and black, in particular) is also evident by observing the surface of the mock-up by a stereomicroscope (Fig. 4d), although information on their position within the coating system is not accessible by the stereomicroscope without sampling.

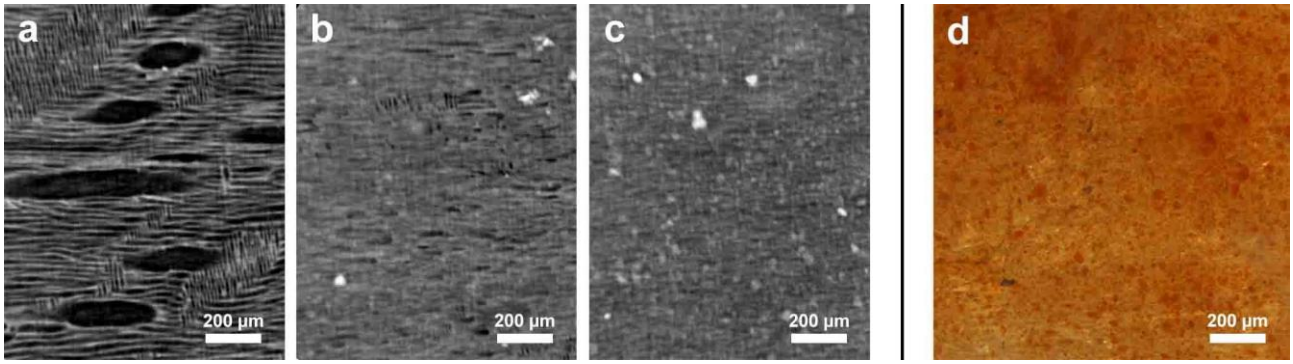

Figure 4. Radial slices from Madder1 (slice planes are reported in Fig. 3c); a) the porous wood under the coating system; b) the ground layer clogging the wood porosity. Some bright particles (possibly sandpaper residues) are evident; c) the dispersion of the lake particles; d) the surface of Madder1 observed through a stereomicroscope under visible light.

The overall results obtained on the mock-ups have highlighted the expected appearance of the various particles and the merits of the transverse, tangential and radial slices. Therefore, they have been used as a guide when examining the reconstructed volume of the historical fragment. By scanning the mock-ups we obtained a preliminary demonstration that specific morphologies can be related to known situations. Therefore the SR-micro-CT scans can be extremely useful for the preliminary interpretation of the finishing treatments.

3.2 Fragment from a cello by Andrea Guarneri

The fragment detached from the front plate of a cello by Andrea Guarneri has been considered in order to evaluate the performances of the SR-micro-CT scan for interpreting a real coating system from a historical musical instrument. The chemical information already obtained for this fragment, reported in Fiocco et al [5] and briefly summarised in section 2.2, has been considered for an overall discussion of the tomographic images.

Samples detached from this fragment were mounted in cross section and imaged by OM (Fig. 5a) and by SEM in back scattered electron mode (Fig. 5b). The images show the presence of three layers and are considered for qualitative comparison with the slices obtained by the SR-micro-CT scan.

The proteinaceous ground layer (A in Fig. 5a,b) - and the particles embedded in it - are clearly visible in the images obtained by OM and SEM. A thin coloured layer (B in Fig. 5a,b) between the ground and the varnish layers is visible by the OM (Fig. 5a), but it is not evident by the SEM image (Fig. 5b), thus indicating a mean atomic composition similar to that of the ground layer.

The varnish layer (C in Fig. 5a,b), prepared with a natural resin, is highlighted by a bright fluorescence under the OM (Fig. 5a) and appears as a darker layer topping the system in the SEM image (Fig. 5b). Very small particles are also visible within the varnish.

A different kind of information derives from the SR-micro-CT scans. The features of the wood are evident by virtually slicing the reconstructed volume, and easily enables the recognition of the characteristic pattern of spruce wood, historically used for the construction of front plates [12] in bowed string instruments.

When the coating system is considered, it is evident that transverse (Fig. 5c) and tangential (Fig. 5d) virtual slices clearly show the penetration of about 200 µm of the ground layer into the porosity of the wood and allow the detection of some bright particles embedded in the ground layer. In particular, Fig. 5c shows the presence of wood inhomogeneities, which have been filled up and flattened by the ground layer embedding the inorganic particles.

The dispersion of fine ochre particles in the varnish (Fig. 5c C) is barely detectable by considering the whole set of transverse and tangential slices, possibly due the low concentration and very small diameter (about 2 µm) of the particles.

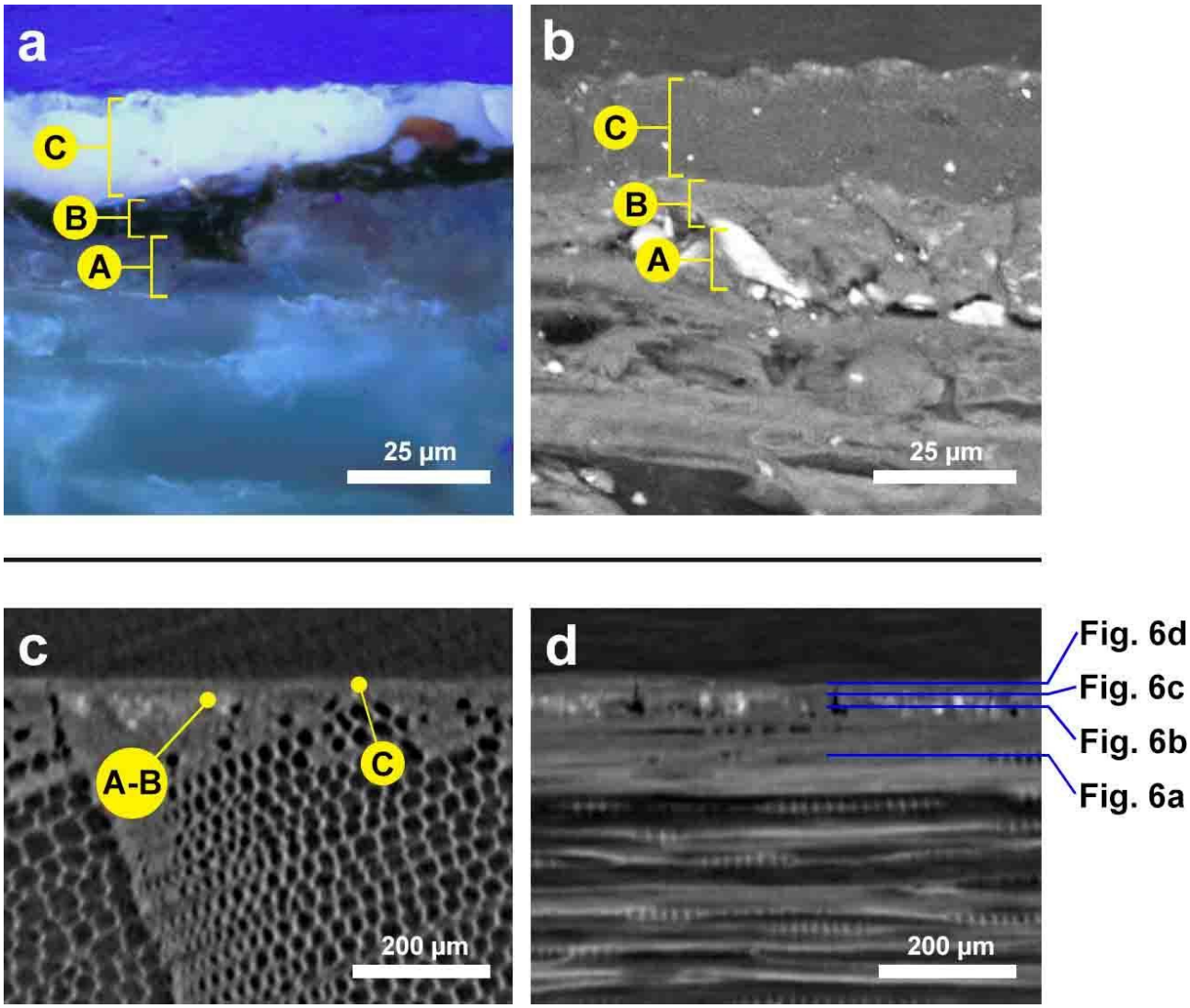

Figure 5. a) Polished cross section from a cello of Andrea Guarneri observed through the OM under UV illumination. Ground layer (A), intermediate coloured layer (B) and varnish (C) are indicated; b) the same cross section observed by SEM in back scattered electron mode. Ground layer (A), intermediate coloured layer (B) and varnish (C) are indicated; c) transverse slice showing the penetration of the ground coat into the wood and the presence of embedded particles. Ground and intermediate coloured layers (A-B) and varnish (C) are indicated; d) tangential slice showing the planes for radial images reported in Fig. 6.

Further information derives from radial virtual slicing of the reconstructed volume (Fig. 6a-d), which show the ground layer that have penetrated the wood surface sealing the porosity (Fig. 6a) and the dispersed particles levelling crackles and inhomogeneities on the wood surface (Fig. 6b). The occurrence of smaller and less bright particles in these slices may indicate the presence of a further thin layer (Fig. 6b), although it cannot be not unambiguously detected by the technique. Furthermore, small and rare particles are highlighted in the varnish (Fig. 6c,d).

A dynamic presentation of the coating system is reported in the supplementary material (Video S2). Nevertheless, similar information can be summarized by an image of the SR-micro-CT reconstructed volume (Fig. 6e) showing the complete sequence of the layers, as derived from the interpretation of slices. The embedded particles - and the dispersing agents - have been coloured to highlight different situations, in order to offer an immediate and exhaustive overview of the coating system.

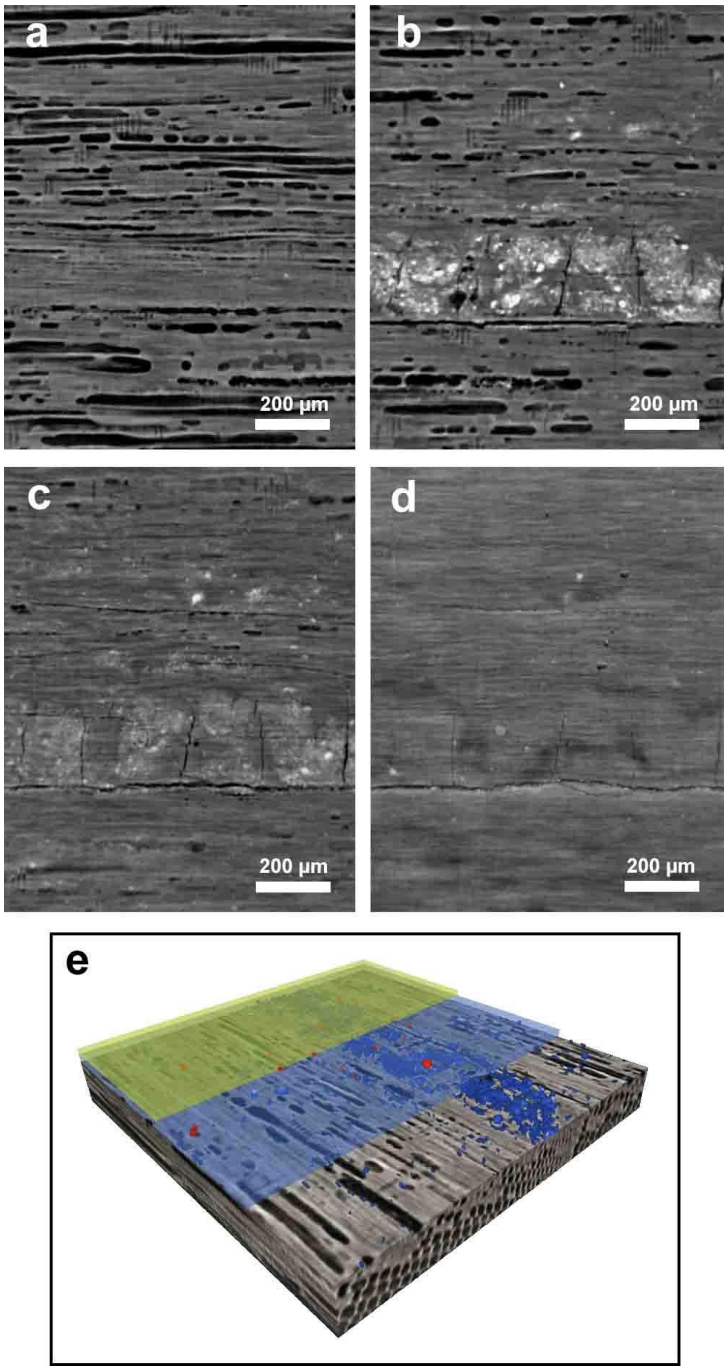

Figure 6. Radial slices from a cello of Andrea Guarneri (slice planes are reported in Fig. 5d); a) The ground layer clogging the porous wood; b) radiopaque particles embedded in the ground layer levelling wood inhomogeneities; c) dispersion of small particles at the ground-to-varnish interface; d) upper varnish embedding rare radiopaque particles; e) virtual reconstruction of the coating system. Particles dispersed in the ground layer are coloured in blue, and the rare particles visible in the varnish are in red. The ground layer and the varnish layers are evidenced in blue and yellow, respectively.

4. Conclusions

By considering the overall set of the SR-micro-CT reconstructed volumes, it is evident that the main morphological features of the finishing layers have been identified both in the mock-ups and in the historical fragment.

The use of different dispersing materials employed to prepare the ground layer and to finish the surface has been highlighted thanks to their (slightly) different radiopacity. In addition, a different interaction with X-rays for different stages of polymerisation in the oil-colophony varnish has emerged from the scans performed on

the (recently prepared) mock-ups. This evidence is possibly irrelevant for the investigation of historical instruments, as relative differences in the polymerization stage of the linseed oil in outer and inners coats tends to zero during time. Nevertheless, it highlights that the SR-micro-CT approach is able to discriminate organic materials with a rather similar composition.
On the other hand, it emerges that some features of the considered coating systems are not highlighted by X-rays in the tomographic scans. In particular, the occurrence of a thin coloured layer in the Guarneri's instrument could not be unambiguously detected in the greyscale images obtained by the SR-micro-CT scans.
The CT scans obviously do not give direct information about the chemical nature of the materials involved in the layers, nevertheless, the visualization - obtained through a non-invasive procedure - of a ground layer under the varnish is a valuable starting point to characterise the technical features of the coating system.
Moreover, radial virtual slices have produced excellent views of the particles dispersed in the whole stratigraphy – useful for interpreting the production procedures - giving a much more representative picture than the one recovered through direct observations on physical cross sections. Furter case-studies shall be considered in order to possibly enlarge the number of historical instruments that will be investigated, as for many of them no sampling is possible.
The method developed in this work is the first step towards a widespread application of SR-micro-CT for the investigation of coating systems in historical bowed string instruments, and will give new impetus to the scanning of further case-studies from the production of early violin makers.

Acknowledgements
The experiments at Elettra have been performed within the proposal n. 20170163. Authors thank Dr. Nicola Sodini for his valuable help in setting up the positioning system at the Synchrotron facility.
The authors are grateful to the International violin making school of Cremona, to M° Alessandro Voltini in particular for providing the fragment of the historical musical instrument and to Dr. Claudio Canevari for preparing the mock-ups.
This scientific research has been generously financed by the Arvedi Buschini Foundation. The support of Università degli Studi di Torino (ricerca locale 2016) and NEXTO project (Progetti di Ateneo 2017) is kindly acknowledged.

References

[1] V. Bucur, In Handbook of Materials for String Musical Instruments, 1st ed. (Springer International Publishing, Switzerland, 2016).

[2] F. Setragno, M. Zanoni, F. Antonacci, A. Sarti, M. Malagodi, T. Rovetta, C. Invernizzi, Acta Acust. Acust., 103 (2017).

[3] J.P. Echard, B. Lavédrine,. J. Cult. Herit., 9 (2008).

[4] C. Invernizzi, A. Daveri, T. Rovetta, M. Vagnini, M. Licchelli, F. Cacciatori, M. Malagodi, Microchem. J., 124 (2016).

[5] G. Fiocco, T. Rovetta, M. Gulmini, A. Piccirillo A., M. Licchelli, M. Malagodi, Appl. Spectrosc., 71 (2017).

[6] C. Invernizzi, G.V. Fichera, M. Licchelli, M. Malagodi, Microchem J., 138 (2018).

[7] J.P. Echard, Spectrochim. Acta B, 59, 10-11 (2004).

[8] J.P. Echard, L. Bertrand, A. von Bohlen, A.-S.L. Hô, C. Paris, L. Bellot-Gurlet, B. Soulier, A. Lattuati-Derieux, S. Thao, L. Robinet, B. Lavédrine, S. Vaiedelich, Angew. Chem., 49, 1 (2010).

[9] C. Invernizzi, A. Daveri, M. Vagnini, M. Malagodi, Anal. Bioanal. Chem., 409 (2017).

[10] T. Rovetta, C. Invernizzi, M. Licchelli, F. Cacciatori, M. Malagodi, X-Ray Spectrom., 47, 2 (2018).

[11] G.V. Fichera, T. Rovetta, G. Fiocco, G. Alberti, C. Invernizzi, M. Licchelli, M. Malagodi, Microchem J., 137 (2018).

[12] B. Brandmair, P.S. Greiner, Stradivari Varnish, 1st ed. (B. Brandmair, Munich, 2010).

[13] B.H. Tai, J. Violin Soc. Am., 21 (2007).

[14] G. Fiocco, T. Rovetta, M. Gulmini, A. Piccirillo, C. Canevari, M. Licchelli, M. Malagodi, Coatings, 8, 5 (2018).

[15] J.P. Echard, M. Cotte, E. Dooryhee, L. Bertrand, Appl. Phys. A-Mater., 92, 1 (2008).

[16] S.A. Sirr, J.R. Waddle, Radiology, 203 (1997).

[17] T. Borman, B. Stoel, J. Violin. Soc. Am., 22 (2009).

[18] L. Mancini, G. Tromba, F. Zanini, J. Neutron Res., 14 (2006).

[19] J. Kaiser, L. Reale, A. Ritucci, G. Tomassetti, A. Poma, L. Spanò, A. Tucci, F. Flora, A. Lai, A. Faenov, T. Pikuz, L. Mancini, G. Tromba, F. Zanini, Eur. Phys. J., 32D (2005).

[20] A. Snigirev, I. Snigireva, V. Kohn, S. Kuznetsov, I. Schelokov, Rev. Sci. Instrum., 66 (1995).

[21] N. Sodini, D. Dreossi, R.C. Chen, F. Fioravanti, A. Giordano, P. Herresthal, L. Rigon, F. Zanini, J. Cult. Herit., **13S**, S44-S49 (2012).

[22] F. Zanini, The Strad, 123 (2012).

[23] N. Sodini, D. Dreossi, A. Giordano, J. Kaiser, F. Zanini, T. Zikmund, J. Cult. Herit., 275, S88-S92 (2017).

[24] S. Tirat, I. Degano, J.P. Echard, A. Lattuati-Derieux, A. Lluveras-Tenorio, A. Marie, S. Serfaty, J.Y. Le Huerou, Microchem. J., 126 (2016).

[25] J. Kirby, M. Spring, M. Higgitt, National Gallery Technical Bulletin, 26 (2005).

[26] P. Cloetens, M. Pateyron-Salome, J.Y. Buffière, G. Peix, J. Baruchel, F. Peyrin, M. Schlenker, J. App. Phys., 81 (1997).

[27] F. Brun, L. Massimi, M. Fratini, D. Dreossi, F. Billé, A. Accardo, R. Pugliese, A. Cedola, Adv. Struct. Chem. Imag., 3, 1 (2017).

[28] F. Brun, A. Accardo, G. Kourousias, D. Dreossi, R. Pugliese, Proceedings of the International Symposium on Image and Signal Processing and Analysis (ISPA 2013), Trieste, 2013, edited by G. Ramponi, S. Lončarić, A. Carini, K. Egiazarian (IEEE, Trieste, 2013).

[29] D. Paganin, S.C. Mayo, T.E. Gureyev, P.R. Miller, S.W. Wilkins, J. Microsc. 206 (2002).

[30] G.T. Herman, Image Reconstruction from Projections: The Fundamentals of Computerized Tomography, 1st ed. (Academic Press, New York, 1980).